Opto-Electronics Review

journal homepage: publishinghouse.pan.pl/opelre



Identifying heat transfer problems during vacuum anodic bonding by thermal imaging measurements

Tomasz Grzebyk, Paweł Urbański*, Krzysztof Stojek

Faculty of Electronics, Photonics and Microsystems, Wroclaw University of Science and Technology,
ul. Janiszewskiego 11/17, 50-372 Wrocław, Poland

Article info

Article history:
Received 16 Jun. 2026
Received in revised form 18 Aug. 2026
Accepted 04 Sep. 2026
Available online 21 Oct. 2026

Keywords:
anodic bonding;
heat transfer;
microsystem technology;
thermal imaging.

Abstract

Vacuum anodic bonding is widely applied for hermetic packaging of microelectro-mechanical (MEMS) devices; however, obtaining reliable high-quality bonds under vacuum conditions remains challenging. We have assumed that main reason for that is reduced heat transfer between bonded structures and a heating stage. To prove that we have investigated thermal phenomena occurring during vacuum anodic bonding using infrared thermography, temperature of silicon and silicon-glass structures was continuously monitored during heating, evacuation, and pressurisation of a custom-built vacuum bonding system. The measurements revealed that, after reaching high vacuum, the temperature of bonded elements decreased by approximately 40–60%, despite only minor changes in the hot plate temperature. The effect was observed for both single-layer and multilayer structures and was attributed to the disappearance of gas-assisted heat transfer under vacuum conditions. The obtained results explain the low ion currents and reduced bonding efficiency frequently observed during vacuum anodic bonding. Based on experimental observations, several practical approaches for improving heat transfer were proposed. Their implementation increased the bonding yield from approximately 25% to 75%. The presented methodology provides a useful diagnostic tool for optimising vacuum anodic bonding processes and improving the reliability of MEMS packaging.

1. Introduction

Anodic bonding is one of the most frequently used processes applied in micro-electro-mechanical system (MEMS) technology. In this process, silicon and borosilicate glass substrates can be irreversibly connected [1, 2]. It is often used as the last step of fabrication for encapsulation of miniature devices.

From a technical point of view, three factors must be ensured to perform it correctly: proper surface pretreatment (cleaning, hydrophilisation), high temperature (preferably 450 °C), and high voltage (e.g., 1500 V). The mechanism is well understood and described in detail elsewhere [3–6]. Here, the last two factors drive ion flow within the borosilicate glass, which is essential for the process.

Depending on the final conditions, which should be ensured inside a MEMS package, the process can be carried out:

- on a laboratory desk, in contact with the atmosphere,
- in an environmental chamber filled with a chosen gas or a mixture,
- in vacuum conditions.

Performing atmospheric processes is relatively easy, ion currents are high, as long as the structures are clean, the bonding interface will be good quality. The most problematic is the high vacuum bonding, applied to encapsulate devices which require such conditions for proper operation. It must ensure a very tight connection, which will prevent external gas leakages.

Our group is specialised in designing high vacuum MEMS: including X-ray sources, electron microscopes or mass spectrometers [7–9]. Although we were able to manufacture vacuum-tight devices, the technological yield was at unsatisfactory level. Many structures after the last vacuum bonding process were not hermetically sealed, and the pressure often rose rapidly up to atmospheric level.

*Corresponding author at: pawel.urbanski@pwr.edu.pl

https://doi.org/10.24425/opelre.2026.7471
1896-3757/ Association of Polish Electrical Engineers (SEP) and Polish Academy of Sciences (PAS). Published by PAS
© 2026 The Author(s). This is an open access article under the CC BY license (https://creativecommons.org/licenses/by/4.0/).

We wanted to investigate what was the real cause of the problems, thus we have studied the vacuum anodic bonding process more deeply, concentrating mostly on thermal issues.

Infrared thermography (IRT) has become an important diagnostic tool in electronic engineering owing to its ability to provide fast, non-contact and full-field temperature measurements. It is widely used for thermal characterisation of electronic components and packages, hotspot detection, reliability assessment and evaluation of heat transfer phenomena. Recent studies have demonstrated the usefulness of IRT in analysing thermal behaviour of electronic assemblies and advanced packaging technologies [10–12]. However, to the best of our knowledge, its application to direct temperature measurements during vacuum anodic bonding has not yet been reported. Therefore, in this work, IRT was employed to investigate heat transfer mechanisms occurring during this process.

2. Experimental set-up

The anodic bonding can be performed in specialised bonders [13–15], which are commercially available, but usually very expensive and dedicated for connecting whole several-inch wafers. In many situations, especially at prototyping stage, during laboratory-scale MEMS packaging or when the structures are very complex, commercial set-ups cannot be utilised. In many experiments, we bond structures consisting of multiple pre-bonded silicon and glass layers, forming non-planar assemblies, with neighbouring elements located at different heights. Such cases require preparation of custom-built bonding stations.

Our set-up consists of a $30 \times 30 \times 30$ cm^3 vacuum chamber (Fig. 1) connected to a roughing and turbo-molecular pump, which ensures up to 10^{-6} hPa. The system is equipped with a heated table (hot plate, serving as a bottom electrode) with 4 cartridge heaters. Its temperature is measured by a thermoresistor Pt100 placed inside the hot plate. The chamber possesses also a vacuum manipulator with a clamp for manipulating silicon and glass elements, another linear-rotary manipulator which moves the top electrode and an optical window at the top wall allowing for visual inspection.

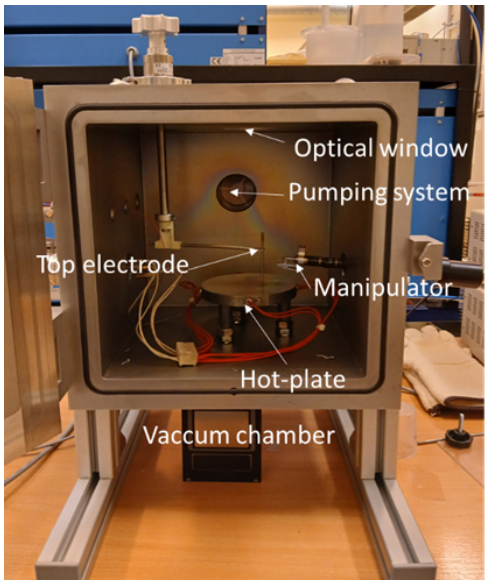


Fig. 1. Vacuum bonding system applied in the experiments.

Usually, the bottom part of a MEMS structure (which can have a form of a single silicon or glass element or more sophisticated designs composed of several silicon and glass elements connected earlier in the atmosphere) is placed directly on the hot plate. The upper part (usually a silicon lead) is being held in a clamp of a vacuum manipulator. The hot plate is turned on, and the elements are heated up to 450 °C. Then, the vacuum chamber is evacuated, the silicon lead is placed onto the bottom part in a proper position, a top electrode is placed onto it (no additional force is applied) and the bonding process is performed.

It has been observed that the ion currents measured during the vacuum bonding are much smaller than registered in the same configuration when the process takes place in the atmospheric pressure. Since visual inspection is not possible either, it is hard to determine exactly when the process is finished. Thus, in most cases, the bonding is performed during a constant time, equal to 7 min. The tightness is assessed after the whole process is finished – when structures are taken out of the vacuum chamber. As mentioned earlier, in many cases it appears that some leakage is observed.

The most probable factor which leads to the problems with the vacuum bonding was expected to lie in thermal issues. We suspected that the temperature of the elements, especially if these were multilayer structures, could be lower than the temperature of the hot plate, which reduced the ion flow in the glass substrates.

In the reported experiments, the authors tried, for the first time to their knowledge, to investigate the real temperature of silicon-glass elements during vacuum anodic bonding. We assumed that the most credible results can be obtained thanks to the use of thermal imaging camera [16]. Such approach ensures quantitative, contactless, rapid analysis with high sensitivity and resolution [17]. These factors cause thermography to be a common method applied in many fields: from medicine [18], industry [19, 20], to civil engineering [21]. This method allows to observe continuously how the temperature of each element changes in time in contactless configuration, especially during evacuation of the chamber. However, to apply thermal imaging for objects inside a vacuum chamber, few technical issues had to be solved first [22].

The first problem is that the glass window applied in the vacuum chamber prevents infrared radiation from reaching the camera. It was replaced with a silicon wafer attached to the vacuum system on the special flange (Fig. 2). Both the silicon window and the flange itself cause some attenuation of the signal, but this effect was taken into account and corrected before proper measurements. The second problem is the low emissivity of silicon and glass elements Before placing the samples inside the vacuum system, their surfaces were partially coated with Helling 3D Scan Spray to obtain a uniform emissivity of 0.98. The coating was applied according to the manufacturer's recommendations by spraying several thin layers onto the surface, with sufficient time between applications to allow the solvents to evaporate. It is crucial for precise determination of temperature based on the IR measurements.

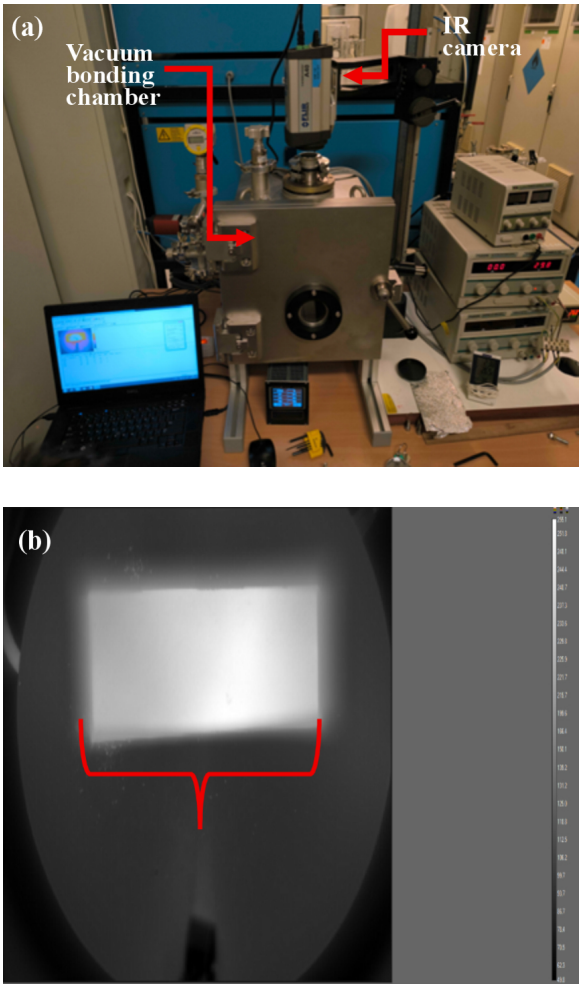


Fig. 2. Vacuum system with a thermal imaging camera applied (a), calibration element covered with an antiglare coating registered with the camera (b).

3. Experiments

In the proper experimental stage, we have concentrated on measuring the temperature of several single and multilayer silicon and glass elements during evacuation and pressurisation of the vacuum station.

The temperature varied only in the range from 20 up to 200 °C due to the thermal stability limits of the antiglare coating used for thermographic measurements. The upper temperature is twice lower than applied usually during the bonding, but most of the relations recorded during the measurements would remain very similar also in higher temperatures.

During the experiments, the temperature was controlled mostly by the thermal imaging camera FLIR A40m. Apart from that, we had also an insight into the readings of a Pt100 sensor placed inside the hot plate. Thermal measurements system was calibrated before the experiments – that means the apparent (sometimes called reflected) temperature was determined. At first, we measured distance between the camera and the measurement plane (0.4 m). Then, we measured the relative humidity (36%) and the atmospheric temperature (27.0 °C). These factors allowed to determine the amount of energy that was absorbed by the atmosphere. To determine apparent temperature, a crumpled aluminium foil was placed in the measurement plane. Setting the foil emissivity to 1 disables temperature correction caused by IR reflections.

The proper experimental stage started with the characterisation of 3 samples: silicon, silicon covered with an antiglare coating, and silicon connected to glass plate [Fig. 3(a)]. Temperature was monitored at their surfaces and additionally at the surface of the hot plate. The initial temperature of all 1–2 layers elements was almost equal to the temperature of the hot plate (~200 °C). At time equal to 0, the vacuum set-up was turned on. During the first period (3 min), pressure gradually decreased down to about 1 hPa, no significant changes in the temperature were noticed [Fig. 3(b)]. However, when a turbomolecular pump was turned on (beginning of stage 2), and pressure dropped rapidly to 10^{-4} hPa, a sudden decrease of temperature of all elements was recorded by the IR camera (up to 120 °C), the most intensive for the structure covered with the antiglare coating.

At the same time, the temperature of the hot plate recorded by the camera stood almost constant. However, the one shown by the Pt100 sensor decreased by 50 °C.

We believe that these effects are mainly attributed to the high thermal contact resistance (TCR) between the hot plate and the silicon/glass structures [23, 24]. Due to the microscopic roughness of both contact surfaces (Fig. 4), the real contact area is much smaller than the apparent one. Under atmospheric pressure, the remaining gaps are filled with gas, which significantly contributes to heat transfer. However, under high vacuum conditions, this contribution disappears, making thermal contact resistance the dominant factor limiting heat transport between the hot plate and the bonded structures [25].

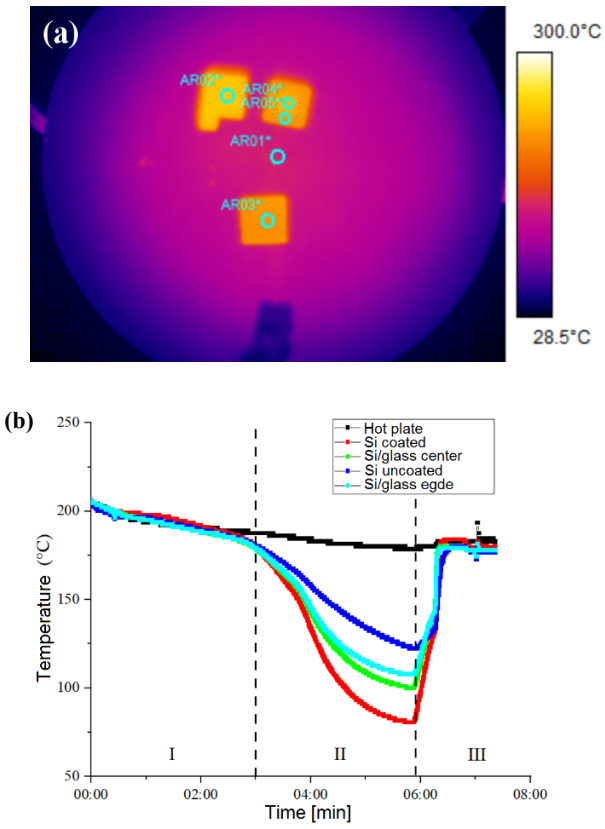


Fig. 3. Silicon and glass elements laying on a hot plate monitored with thermal imaging camera (a) and the change of temperature during evacuation and pressurisation of the vacuum set-up recorded by the camera (b).

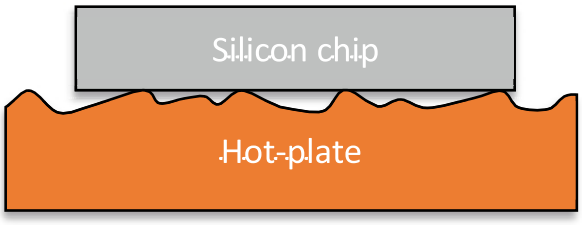


Fig. 4. Schematic, magnified view of a silicon chip lying on a hot plate.

Under atmospheric pressure, or even if it is reduced to 1 hPa, the space between the hot plate and the element lying on it is filled with gas molecules. They are responsible for heat transfer. When mean free path of gas molecules is smaller than the real distance between two objects, a transition from continuum to rarefied gas heat transfer regimes occurs. In this regime, gas particles stop contributing to heat transfer and energy can be transmitted almost solely by the radiation. Thus, it is much harder to heat up any element.

What are the consequences of this result? The first one is that any measurements of temperature with a thermo-resistor performed in vacuum have reduced value. The differences in the temperatures between the camera and Pt100 readings were very big. Situation has not changed much even if sensor was pushed against the hot plate surface with a screw. Similar effects might be present in all other TVAC experiments, and it is very important to be aware of it. Sintering of the sensor to the substrate (which was not done in this case) can improve the situation – filing imperfect contact surfaces with highly conductive thermal interface material (TIM) should efficiently improve heat flow [26–28]. Additionally, sintered joints can operate in such relatively temperatures as 450 °C [29–31]. However, similar approach cannot be used to silicon and glass elements during anodic bonding. Their surfaces must stay clean, and they cannot be directly connected to a hot plate.

The second conclusion is that the thermography seems to be the best method for contactless, independent on other factors, undisrupted measurements, which allows to record real temperature of all elements present in the vacuum chamber.

The third fact, most important in terms of anodic bonding, is that heating of any elements just by placing them on a hot plate is very hard when performed in vacuum conditions. Due to high thermal conductivity and convection of air, the bonded elements under atmospheric pressure have the same temperature as the hot plate. But in vacuum, when mentioned mechanisms are significantly reduced, the only process which leads to heat transfer is radiation. Moreover, the elements not only absorb energy from the hot plate but also emit part of it into the surroundings. It is visible especially when comparing a pure silicon chip and the chip covered with the antiglare coating. The second one, which has higher emissivity, exhibited twice higher temperature loss than uncovered chip.

From the measurement point of view, it is a drawback of thermal imaging method, because it causes changes of the temperature of the examined sample. However, it can be minimised by depositing the antiglare coating only on a small (1 mm^2) spot on each element. It still ensures reliable measurements of the temperature and at the same time it does not artificially increase heat dissipation. Such an approach was utilised in the next measurements.

In the second experiment, we have concentrated on two additional aspects: how the thickness of bonded structures affects their temperature during the evacuation process and whether it is possible to counteract the significant temperature loss. This time MEMS structures consisting of 1 to 7 silicon/glass layers were examined [Fig. 5(a)].

At ambient pressure, the thicker the structure the temperature was slightly lower, but it did not drop below 160 °C [Fig. 5(b)].

This time the evacuation of the vacuum chamber was conducted in two ways. The regulator responsible for the temperature control could be turned off when evacuation starts, as in the first experiment, or it could be turned on continuously (in this case, each time the temperature at PT100 drops below 200 °C, it turns on the heating elements – in practice, it was turned on during the whole evacuation process).

It might be a bit surprising that the structures which were thicker, although they had lower temperature at the beginning of pumping process, when high vacuum was obtained, their temperature was higher than that of the thinner ones. This can be explained by the higher heat capacity, which allows the temperature to stay for a longer time.

What is also very important and unexpected is the fact that, independently of the hot plate temperature, it was impossible to heat the MEMS elements to the initial

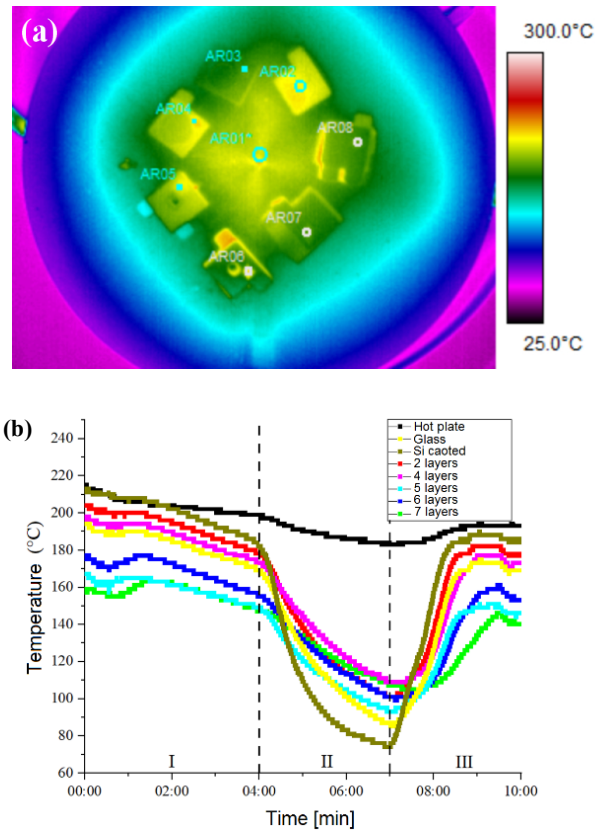


Fig. 5. Multilayer silicon-glass chips laying on a hot plate monitored with thermal imaging camera (a) and the change of temperature during evacuation and pressurisation of the vacuum set-up with a regulator turned off during the process (b).

temperature once high vacuum was obtained. If the temperature regulator was continuously turned on, the heating element kept increasing its temperature (it is visible on a thermal image, Fig. 5, but not on the Pt100 sensor – which showed all the time temperature below 200 °C).

The temperature of the hot plate after 8 min reached almost 300 °C. Even such high temperature was not sufficient to heat silicon and glass elements back to 200 °C.

We also investigated what happened when the chamber was pressurised. The rapid increase of pressure increases the thermal conductivity through the gas, which is crucial for the overall heat transfer and structures are rapidly heated up by the hot plate. It is also visible that the temperature of the hot plate is almost as high as at the beginning of the experiment [in the case when regulator was turned off, [Fig. 5(b)], and much higher than 250 °C when regulator was turned on (Fig. 6). It proves once again that the problem lies not with a heating element, but with a very poor heat transfer between the hot plate and silicon and glass elements.

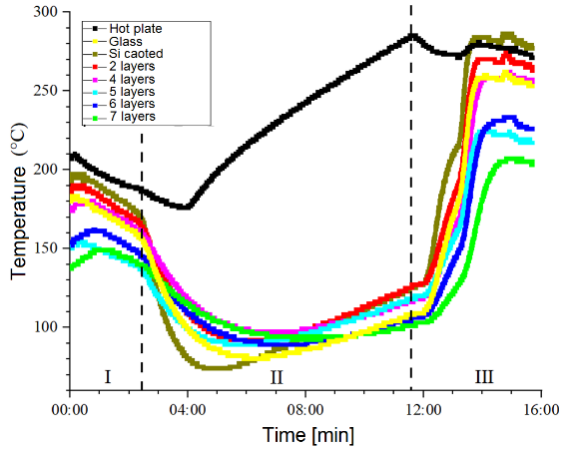


Fig. 6. The change of temperature during evacuation and pressurisation of the vacuum set-up with regulator turned on continuously.

How would these observations affect typical bonding processes? And what would change in 450 °C? It is hard to say precisely: heat conductance and convection scales linearly with temperature, radiation with T^4. If temperature of the elements was reduced by 40–50% during gas evacuation at 200 °C, it can be estimated that it should be at the level of 250–300 °C, when hot plate is set to 450 °C.

In such low temperature, the ion conductivity is very small, that is why the currents recorded during the bonding are so small, and therefore the probability of conducting successful process is low.

What actions could be undertaken to improve the situation? One can:

- improve heat transport by improving the microscopic contact between the elements, e.g., by precise polishing of the hot plate surface,
- decrease the radiation losses of the connected elements, e.g., by adding a heater above the structure or using reflectors,
- replace the top electrode with one having higher heat capacity. Before bonding, it can be heated to 450 °C and then placed onto the bonded structure to provide additional heat or reduce radiation losses.

Due to its technical simplicity, the last method was applied in practice. The vacuum bonding yield increased from approximately 25% to 75%, indicating that improving the thermal conditions can significantly improve the bonding process.

4. Conclusions

The research presented is valuable for two major reasons. First of all – from metrological point of view – it has been shown that thermographic method can be successfully applied to measure and analyse processes taking place inside a vacuum system as long as proper adjustments of the system and proper calibration are done. The main advantage of this method is that it enables non-contact and spatially resolved temperature measurements not sensitive to heat transfer problems.

Second, even more important aspect is that the conducted experiments allowed to find a true cause of problems with performing vacuum anodic bonding and find a solution to it. It was demonstrated that thermal issues, especially poor heat transfer between the heating element and the silicon and glass chips, are important factors affecting vacuum anodic bonding yield. This results in fact that bonded elements reach temperatures significantly lower than the temperature of the hot plate, which reduces the ion current and bonding strength. Reducing the heat dissipation or addition of another heat source from the top of the structure can cause significant improvement to the process.

Acknowledgements

The work was financed by the projects no. 2021/41/B/ST7/01615 and 2023/49/B/ST7/01949 of Polish National Science Centre.

Paweł Urbański's work was financially supported by the Foundation for Polish Science START Award.

References

[1] Lapadatu, A. C. & Jakobsen, H. Anodic Bonding. in *Handbook of Silicon Based MEMS Materials and Technologie, 2nd ed.* 599–610 (Elsevier, 2015). https://doi.org/10.1016/B978-0-323-29965-7.00030-0

[2] Xu, J., Du, Y., Tian, Y. & Wang, C. Progress in wafer bonding technology towards MEMS, high-power electronics, optoelectronics, and optofluidics. *Int. J. Optomechatronics* **14**, 94–118 (2020). https://doi.org/10.1080/15599612.2020.1857890

[3] Dziuban, J. A. *Bonding in Microsystem Technology*. (Scholars Portal, 2019).

[4] *Handbook of Silicon Based MEMS Materials and Technologies*. (Eds. Tilli, M. *et al.*) (Elsevier, 2020). https://doi.org/10.1016/C2018-0-01845-9

[5] Knechtel, R. & Schwarz, U. Wafer Bonding in MEMS Technologies. in: (eds. Zentner, L. & Strehle, S) *Microactuators, Microsensors and Micromechanisms MAMM 2020. Mechanisms and Machine Science* 96, 89–102 (Springer, 2021). https://doi.org/10.1007/978-3-030-61652-6_8

[6] Tanaka, S. Wafer-level hermetic MEMS packaging by anodic bonding and its reliability issues. *Microelectron. Reliab.* **54**, 875–881 (2014). https://doi.org/10.1016/j.microrel.2014.02.001

[7] Krysztof, M., Bialas, M., Grzebyk, T. & Gorecka-Drzazga, A. Atmospheric pressure electron detection method for MEMS

Electron microscope. *IEEE Electron Device Lett.* **43**, 813–815 (2022). https://doi.org/10.1109/LED.2022.3162950

[8] Urbański, P. & Grzebyk, T. Detection system for a miniature MEMS X-ray source. *Opto-Electron. Rev.* **31**, 147038 (2023). https://doi.org/10.24425/opelre.2023.147038

[9] Szyszka, P. *et al.* MEMS quadrupole mass spectrometer. *Sens. Actuators B Chem.* **411**, 135712 (2024). https://doi.org/10.1016/j.snb.2024.135712

[10] Furtado Paes, V., Nascimento Rosa, J., Bastos Costa, P., Magalhães Ferreira, R. A. & Porto, M. P. Calibration of a cooled MWIR camera with a narrow-band filter for quantitative thermography. *Quant. Infrared Thermogr. J.* **23**, 174–193 (2026). https://doi.org/10.1080/17686733.2025.2556525

[11] Lin, R. *et al.* Enhancing surveillance in parking lots: A thermal infrared approach to human action recognition. *Quant. Infrared Thermogr. J.* **23**, 12–29 (2026). https://doi.org/10.1080/17686733.2025.2494871

[12] Mendez-Bohorquez, M.-D., Ebert, J., Sommerlade, L., Schmoll, R. & Kroll, A. The size of source effect for middle- and long-wavelength infrared cameras: assessment by direct measurements and a modulation transfer function approach. *Quant. Infrared Thermogr. J.* **23**, 1–18 (2025). https://doi.org/10.1080/17686733.2025.2589712

[13] Ayumi. Overview of anodic bonding equipment. *Ayumi Co., Ltd.* http://www.ayumi-ind.co.jp/en/products/vacuum_equipment/setugousouchi/youkyokusetugousoutinogaiou/

[14] EVG. Anodic Bonding. Anodic bonding for interlayer free Si-glass bonding. *EVGroup*. https://www.evgroup.com/technologies/anodic-bonding

[15] Inseto. Wafer bonding methods. *Inseto Advanced Technology for Research and Industry.* https://www.inseto.com/wafer-bonding-methods/

[16] Kowalski, Ł., Bembenek, M., Uhryński, A. & Bajda, S. Comparative study of experimental thermographic data and finite element analysis on temperature evolution of PET-G layer deposition during additive manufacturing process. *Bull. Pol. Acad. Sci. Tech. Sci.* **72**, 147926 (2023). https://doi.org/10.24425/bpasts.2023.147926

[17] AL-Jubori, H. N., AL-Darraji, I. & Jerbi, H. Defect detection using thermography camera techniques: A review. *Al-Khwarizmi Eng. J.* **20**, 70–88 (2024). https://doi.org/10.22153/kej.2024.03.002

[18] Kesztyüs, D., Brucher, S., Wilson, C. & Kesztyüs, T. Use of infrared thermography in medical diagnosis, screening, and disease monitoring: A scoping review. *Medicina (B. Aires).* **59**, 2139 (2023). https://doi.org/10.3390/medicina59122139

[19] Zhao, X. *et al.* Progress in active infrared imaging for defect detection in the renewable and electronic industries. *Sensors* **23**, 8780 (2023). https://doi.org/10.3390/s23218780

[20] He, Y. *et al.* Infrared machine vision and infrared thermography with deep learning: A review. *Infrared Phys. Technol.* **116**, 103754 (2021). https://doi.org/10.1016/j.infrared.2021.103754

[21] Garrido, I., Solla, M., Lagüela, S. & Rasol, M. Review of infrared thermography and ground-penetrating radar applications for building assessment. *Adv. Civ. Eng.* **2022**, 5229911 (2022). https://doi.org/10.1155/2022/5229911

[22] Stojek, K. J., Felba, J., Nicolics, J. & Wołczyński, D. Impact of convection on thermographic analysis of silver based thermal joints. *Solder. Surf. Mt. Technol.* **32**, 241–246 (2020). https://doi.org/10.1108/SSMT-11-2019-0040

[23] Zhou, Y. *et al.* Recent advances in thermal interface materials. *ES Mater. Manuf.* **7**, 4–24 (2020). https://doi.org/10.30919/esmm5f717

[24] Wei, B. *et al.* Thermal interface materials: From fundamental research to applications. *SusMat* **4**, e239 (2024). https://doi.org/10.1002/sus2.239

[25] Sauer Jr., H. J. & Sheffield, J. W. Thermal Contact Resistance (TCR)/Thermal Contact Conductance (TCC). in *HEDH Multimedia* (Begellhouse, 2011). https://doi.org/10.1615/hedhme.a.000164

[26] Felba, J. Technological aspects of silver particle sintering for electronic packaging. *Circuit World* **44**, 2–15 (2018). https://doi.org/10.1108/CW-10-2017-0060

[27] Stojek, K. *et al.* Metalization Impact on Heat Transfer Through Sintered Nano-silver-Based Thermal Joints. in *2019 22nd European Microelectronics and Packaging Conference & Exhibition (EMPC)* 1–4 (IEEE, 2019). https://doi.org/10.23919/EMPC44848.2019.8951879

[28] Stojek, K. J. *et al.* Thermal and mechanical analysis of low-temperature and low-pressure silver-based sintered thermal joints. *Solder. Surf. Mt. Technol.* **35**, 9–17 (2023). https://doi.org/10.1108/SSMT-06-2021-0042

[29] Yan, H., Liang, P., Mei, Y. & Feng, Z. Brief review of silver sinter-bonding processing for packaging high-temperature power devices. *Chin. J. Electr. Eng.* **6**, 25–34 (2020). https://doi.org/10.23919/CJEE.2020.000016

[30] Bai, J. G., Yin, J., Zhang, Z., Lu, G.-Q. & van Wyk, J. D. High-temperature operation of SiC power devices by low-temperature sintered silver DIE-attachment. *IEEE Trans. Adv. Packag.* **30**, 506–510 (2007). https://doi.org/10.1109/TADVP.2007.898628

[31] Hutzler, A., Tokarski, A., Kraft, S., Zischler, S. & Schletz, A. Increasing the Lifetime of Electronic Packaging by Higher Temperatures: Solders *vs*. Silver Sintering. in *2014 IEEE 64th Electronic Components and Technology Conference (ECTC)* 1700–1706 (IEEE, 2014). https://doi.org/10.1109/ECTC.2014.6897526